Energy, Mines and Resources Canada | Énergie, Mines et Ressources Canada

CANMET

Canada Centre for Mineral and Energy Technology | Centre canadien de la technologie des minéraux et de l'énergie

ZINC-ALUMINUM FOUNDRY ALLOYS - PROGRESS REPORT NO. 1

M. SAHOO and L.V. WHITING
METALLURGY and FOUNDRY SECTIONS

JUNE 1983

MINERALS RESEARCH PROGRAM

38 pp

PHYSICAL METALLURGY RESEARCH LABORATORIES
REPORT: MRP/PMRL 83-43(TR)

355

PHYSICAL METALLURGY RESEARCH LABORATORIES

REPORT MRP/PMRL 83-43(TR)

ZINC-ALUMINUM FOUNDRY ALLOYS - PROGRESS REPORT NO. 1

by

M. Sahoo and L.V. Whiting

ABSTRACT

Foundry characteristics and mechanical properties of the new family of Zn-Al foundry alloys containing 8, 11 and 27% Al have been examined. These alloys are found to possess excellent fluidity, and thin sections can be easily cast. It is shown that the "underside shrinkage" observed on the bottom face of the castings can be minimized by employing suitable gating ratios and/or titanium modification. However, titanium modification did not improve the mechanical properties of the alloys. The microstructure of the alloys has been characterized by optical and scanning electron microscopy.

RAPPORT PROVISOIRE N° 1 SUR LES ALLIAGES DE FONDERIE ZINC-ALUMINIUM

par

M. Sahoo et L.V. Whiting

RÉSUMÉ

On a fait l'examen des caractéristiques de fonderie et des propriétés mécaniques de la nouvelle famille d'alliages de fonderie zinc-aluminium contenant 8, 11 et 27% d'aluminium. Ces alliages possèdent une fluidité excellente et il est facile d'en couler de petites sections. Il est montré que les retassures observées à la surface inférieure de la pièce coulée peuvent être minimisées en employant des sections d'attaques de coulée appropriées et/ou en ajoutant du titane. Cependant l'addition de titane n'a pas amélioré les propriétés mécaniques des alliages. On a finalement défini les caractéristiques de la microstructure des alliages par microscopie optique et par microscopie électronique à balayage.

INTRODUCTION

The original Zn-Al alloy developed for sand casting and general foundry use was introduced in the 1960's as ILZRO-12 by the International Lead Zinc Research Organization. Recently, research at the Noranda Research Centre has lead to the introduction of two additional new alloys; one containing 8% Al and the other containing 27% Al (1,2). The chemical specifications of these three alloys are shown in Table 1.

These alloys can compete effectively with cast iron and some copper- and aluminum-base alloys for many applications. In fact, they have achieved considerable success in the nonferrous foundry industry because of many attractive properties like lower initial cost, superior foundry characteristics, better mechanical properties and reduced cost on subsequent finishing operations. However, they possess poor ductility compared with copper alloys. In the sand-cast condition, the three alloys exhibit the following elongation values: 1-2% for the 8% Al alloy, 1-3% for the 11% Al alloy and 3-6% for the 27% Al alloy. In the case of the 27% Al alloy, ductility can be improved to 8-11% elongation through a simple heat treatment of 3 h at 320°C followed by furnace cooling. However, this heat treatment reduces the tensile strength by 25-30%.

It is hoped that the ductility of the Zn-base foundry alloys can be improved by microstructural modification. Because the fracture path follows the Zn-rich phase, the modifying element(s) should be able to refine this zinc-rich phase. Of the various modifying elements Pb, Sn, Cd, Bi, Hg, In, As, Sb and Tl can cause harmful effects by inducing intergranular corrosion and/or grain coarsening.

An earlier PMRL study determined the effects of small additions of Be, Ti, Mn, Ni, Zr and Li on the structure and mechanical properties of standard Zamak 3 (Zn-4% Al) and Zamak 5 (Zn-4% Al-1% Cu) die casting alloys. Metallographic examination indicated the presence of intermetallic compounds in specimens containing Ti, Mn, Ni and Zr. Alloys modified by Be and Li contained fine dross-type segregates. With respect to mechanical properties, it was concluded that the effects of the elements tested were not beneficial to the Zamak-type alloys although there was some indication that Be might improve elongation. It was suggested that alloys of the higher aluminum content should be investigated to examine the effects of Be, Ti, Mn, Ni, Zr and Li on their structure and mechanical properties (3,4).

The work has three objectives:

(i) to determine whether mechanical properties of the alloys can be improved (elongation increased) by addition of third (or more) elements;

(ii) evaluate the castability of the alloys and optimize gating and risering parameters;

(iii) because of its industrial importance, focus attention on the 27% Al alloy and determine whether shrinkage porosity can be reduced by the addition of other elements.

EXPERIMENTAL PROCEDURE

Materials

99.99% pure Zn, commercial pure (99.5%) or 99.99% pure Al, 99.8% pure Mg and electrolytic tough-pitch Cu were used to prepare the alloys. Titanium was added as Al-6% Ti master alloy. Virgin metals and "in-house" scrap consisting of runners, gates and risers, which are clean and reasonably free of sand, have been used. Use of scrap did not appear to have adverse effects on fluidity.

Melting Practice

Melting was carried out in a push-up induction furnace using clay-graphite crucibles coated with alumina. Because aluminum does not dissolve easily in molten zinc, the general melting practice consisted of melting the aluminum, copper and scrap followed by the addition of zinc. Magnesium was plunged into the melt immediately before lifting the crucible for pouring.

No flux was used at any stage in the melting cycle. The casting temperature varied between 450 and 480°C for the 8% Al alloys, 500 and 530°C for the 11% Al alloys and 520 and 570°C for the 27% Al alloys. Time taken for melting and casting was about 30 min.

Test Castings

The following moulds were cast:

1. fluidity spiral (Fig. 1) and fluidity test pattern (Fig. 2) to study the fluidity of the alloy,
2. Dow test bar (Fig. 3) to determine the tensile properties of the sand-cast alloys,

3. 25 x 152 x 305 mm plates to establish gating and risering techniques and to study casting soundness, and
4. 133 x 203 x 324 mm large blocks to determine the liquidus and solidus temperatures of the alloys.

The green sand moulds were prepared in McConnelsville sand (AFS fineness No. 100) with 6% bentonite, 3.5% moisture and 0.5% proprietary liquid "sand conditioners". The moulds had a permeability of 38 to 45 and a green compressive strength of 38 to 42 kPa. The CO_2 sand moulds were prepared from AFS fineness No. 45 washed silica sand and 4% binder (proprietary sodium silicate).

RESULTS AND DISCUSSION

COMPOSITION

The compositions of the alloys are given in Table 2. There appears to be Fe and Si pick-up in alloys where commercial pure aluminum was used for melting.

It may be noted from Table 2 that in some cases the aluminum content is higher than the specified maximum although the charge calculations were done for the nominal compositions. Common practice in the foundry is to send drillings from the risers for chemical analysis. Work done at the British Non-ferrous Research Association has shown that, in the case of the 11% Al alloys, the top of the riser can be 0.5% richer in aluminum than the bottom of the casting (5). This difference in aluminum content is likely to be higher in the case of the 27% Al alloy because of the wider freezing range.

In order to verify the nature of gravity segregation, aluminum analysis was done at different locations in the 133 x 203 x 324 mm block casting as shown in Fig. 4. A graphite chill was used on the 133 x 324 mm (bottom) face of the casting. As shown in Fig. 4, the difference between the aluminum content at the top of the riser and the nominal composition was about 2.8, 1.2, and 3.9% for the 8, 11, and 27% Al alloys respectively. It is surprising that the Zn-8% Al alloy, which has a freezing range of only 20°C, shows such a large variation in composition. However, these results indicate that one must be careful in taking samples for chemical analysis, and it may be preferable to cast small samples in a permanent mould to obtain nominal chemical compositions.

Figure 4 shows that the drag face in contact with the chill gives the right aluminum conposition for the alloy. The centre of the casting has an aluminum content which is below the nominal composition and the top of the casting and the riser appear to be rich as aluminum. This apparent difference in aluminum content can probably be attributed to the difference in density between the first solid to solidify which is rich in aluminum and the remaining liquid. In order to explain the segregation pattern in Zn-Al alloys, large block castings have been made without any chill on the drag surface. Their aluminum contents are being analyzed.

LIQUIDUS AND SOLIDUS TEMPERATURES

The cooling curves of the three alloys were monitored by embedding type K chromel-alumel thermocouples in the sand-moulds. The data were recorded and plotted on the HP 85 Data Acquisition System with internal cold junction compensation.

The cooling curves for the three alloys are shown in Fig. 5. The liquidus and solidus temperatures and the solidification range for the three alloys are shown in Table 3 together with data obtained from the binary Zn-Al phase diagram. Table 3 shows that the freezing range of each alloy is increased by additions of Cu and Mg. Based on these data, the 8, 11 and 27% Al alloys can be classified respectively as short, medium and long freezing range alloys.

FLUIDITY

To determine the optimum pouring temperature range, the casting fluidity was assessed with a spiral fluidity test and Kondic's fluidity test pattern (6) which gives a measure of the extent to which thin sections can be cast. This test pattern takes the form of four strips of various thicknesses gated from a common runner bar. A typical test casting is shown in Fig. 2.

Figures 6 to 8 illustrate the spiral length and the total strip length as a function of pouring temperature for a number of melts in the three alloys. As expected, the spiral length and the total strip length increase with the pouring temperature. This effect is illustrated in Fig. 9 where fluidity data from Fig. 6 to 8 were replotted as a function of superheat.

Figures 10-12 show the relationship between the strip length and strip thickness for various pouring temperatures. It is apparent from Fig. 10-12 that strip length increases with increasing pouring temperature and

for a given pouring temperature is directly proportional to the strip thickness.

The fluidity data show that thin sections can be cast easily in the three Zn-Al alloys and that for best results, a superheat of 50 to 80°C should be employed for pouring.

CASTING SOUNDNESS

Shrinkage porosity can be expected in the 27% Al alloys because of the long freezing range (~110°C). The casting quality was assessed by casting 25 x 152 x 304 mm plates fed by a 76 mm diam riser (with insulating sleeves) in the centre of the plate. The runners were located in the drag, and the gate and the casting were placed in the cope. A typical casting with the gates and the risers is shown in Fig. 13.

Shrinkage defects were observed on the bottom face (drag side) of the casting instead of the top face (cope side) as is generally the case. As shown in Fig. 14, these defects had a circular pattern below the riser. However, underside shrinkage defects were not observed in the 8 and 11% alloys, but began to appear at an aluminum content of about 15%. It may be noted that some castings obtained from the Cominco Product Research Centre also showed underside shrinkage. However, the severity of such defects decreased when a reduced gate cross-section was used (Fig. 15).

As previous work at PMRL had shown that 0.05% Ti refined the grain size of Zn-Al alloys (7,8), a number of castings were made with different gating ratios and titanium concentrations to assess the effect on underside shrinkage. These results are summarized in Table 4.

Table 4 indicates that the gating ratio plays an important role in controlling casting quality. Further improvements in casting quality can be obtained by titanium modification. A gating ratio of 1:5:3 and a titanium content of 0.05 to 0.1% appear to maximize the improvement in casting quality, although some underside shrinkage defects are still present.

Use of a tapered chill (229 mm long, 152 mm wide and tapered from 19 to 6 mm) and an end riser in melt 2658 produced a sound casting in the chilled area. However, a lot of underside shrinkage was produced in the unchilled area (Fig. 21) which titanium modification did not eliminate. However, use of small end chills (152 x 76 x 25 mm) with a riser at the centre produced radiographically sound castings with no underside shrinkage. This shows the importance of a temperature gradient in eliminating underside shrinkage.

MECHANICAL PROPERTIES

Mechanical properties of the cast-to-size test bars are listed in Tables 5-7 for the three types of alloys. The 8 and 11% Al alloys easily met the tensile properties specified by the manufacturer. However, the manufacturer's suggested yield strength could not be obtained in the as-cast 27% Al alloy. Heat treatment at 320°C reduced the UTS and YS of the 27% Al alloys, and there was no significant improvement in the % elongation as expected from the specifications. This may be attributable to the relatively high Mg content of the alloys tested so far.

Addition of titanium did not improve the % elongation of all three alloys. In fact, in some cases the UTS and YS appear to be adversely affected.

MICROSTRUCTURE

Optical micrographs of the three Zn-Al foundry alloys in the as-cast condition are shown in Fig. 22(a) to (c). The 8 and 11% Al alloys are characterized by aluminum-rich primary dendrites with interdendritic eutectic structure rich in zinc. As can be expected from the phase diagram, the volume fraction of eutectic mixture is less in the 11% Al alloy. The eutectic has a lamellar morphology with an interlamellar spacing that is relatively coarse in the 11% Al alloy.

The Zn-27% Al alloy goes through a peritectic and eutectoid transformation during cooling from the liquid state. The as-cast microstructure contains aluminum-rich primaries, zinc-rich islands of solid solution and the eutectoid transformation products. The eutectoid structure appears to be very fine. Furnace cooling from 320°C increases the amount of eutectoid transformation product [Fig. 22(d)].

Scanning electron microscopy resolves the eutectoid structure of the Zn-27% Al alloys; SEM photomicrographs of the unmodified and titanium modified alloys are shown in Fig. 23(a) to (g). Qualitative analysis using energy dispersive X-ray (EDAX) analysis indicates both the light and dark areas along the grain boundaries [Fig. 23(a)] to be very rich in zinc.

In addition to the spaghetti-like eutectoid structure, lamellar eutectoid microstructures were also observed [Fig. 23(d), (e) and (f)]. Alloy 2594 contained 0.042% Ti, but there was no evidence of any titanium-rich compound in the microstructure. However, as shown in Fig. 23(g), a particle of titanium-rich compound of the type described by Pollard et al. was found

in alloy 2596 (7,8). A particle was very rich in Ti and Al and contained very little Zn. A peak for titanium was not obtained in any other zinc-rich, aluminum-rich or eutectoid areas. The titanium-rich compound has been identified as $Al_5Ti_2Zn_5$ (7,8).

ACKNOWLEDGEMENT

The authors acknowledge the expert technical assistance received from Messrs. D.A. Brown, J. Shields, Y. Lavoie, K. Kleinschmidt and G. Weatherall. Scanning electron microscopy work was done by Mr. V. Chartrand.

REFERENCES

1. Gervais, E., Levert, H. and Bass, M. "The development of a family of zinc-base foundry alloys"; Trans AFS 88:183-194; 1980.

2. Barber, M.J. and Jones, P.E. "A new family of foundry alloys"; Foundry Trade Journal; January 1980.

3. Guttman, H. "The development of improved zinc-base die casting alloys. Phase I: Alloy preparation"; Internal Report PM-R-59-25; Physical Metallurgy Division, Mines Branch, Department of Mines and Technical Surveys, Ottawa, Canada; 1958.

4. Guttman, H. "The development of improved zinc-base die casting alloys. Phase II: The effects of addition elements on the mechanical properties of Zamak type zinc-base die casting alloys"; Internal Report 61-148; Physical Metallurgy Division, Mines Branch, Department of Mines and Technical Surveys, Ottawa, Canada; 1961.

5. Sarkar, S., Gardiner, A.P. and Bates, A.P. "ILZRO 12 in the foundry"; BNFMRA Research Report No. A 1704; 1968.

6. Kondic, V. "A new test for fluidity"; Foundry 87:79-83; 1959.

7. Pollard, W.A., Pickwick, K.M., Jubb, J.T. and Packwood, R.H. "The grain refinement of zinc-aluminum alloys by titanium"; Canadian Metallurgical Quarterly 13:535-543; 1974.

8. Pollard, W.A. "Nucleation in Zn-Al alloys grain refined with Ti"; Canadian Metallurgical Quarterly 13:597-606; 1974.

Table 1 - Nominal specifications chemical compositions (wt %) of zinc-aluminum foundry alloys.

Composition	ZA-8*	ZA-12* (ASTM B-669-80)	ZA-27*
Aluminum	8.0-8.8	10.5-11.5	25-28
Copper	0.8-1.3	0.5-1.25	2.0-2.5
Magnesium	0.015-0.030	0.015-0.030	0.01-0.02
Iron	<0.10	<0.075	<0.10
Lead	<0.004	<0.004	<0.004
Cadmium	<0.003	<0.003	<0.003
Tin	<0.002	<0.002	<0.002
Zinc	Bal	Bal	Bal

*Kidd zinc casting alloys.

Table 2 - Chemical compositions* (wt %) of zinc-aluminum foundry alloys.

Melt No.	Al	Cu	Mg	Fe	Si	Ti
2448	10.6	1.45	0.025	0.025	-	-
2449	12.6	1.22	0.033	0.012	<0.01	-
2456	30.6	2.55	0.037	0.016	0.03	-
2459	29.6	2.26	0.031	0.1	0.03	-
2476	28.9	2.46	0.034	0.084	0.02	-
2482	10.95	1.11	0.027	0.016	<0.01	-
2488	27.50	2.35	0.035	0.096	0.02	-
2494	12.7	1.24	0.036	0.044	0.04	-
2508	8.17	1.18	0.022	0.014	0.01	-
2512	8.71	1.15	0.034	0.009	0.01	-
2516	8.08	1.08	0.032	-	-	-
2520	10.4	1.18	0.032	-	-	-
2527	28.66	2.70	0.039	0.075	0.02	-
2529	11.55	1.33	0.02	0.018	0.02	-
2531	29.12	2.67	0.018	0.1	0.02	-
2537	8.81	1.12	0.023	0.027	0.03	-
2539	11.60	1.06	0.032	-	0.01	-
2543	27.0	1.36	0.037	0.073	0.03	-
2548	27.0	2.13	0.037	0.074	0.02	-
2555	11.7	1.20	0.024	0.049	0.03	-
2558-1	25.5	2.32	0.013	0.11	-	-
2558-2	24.9	2.32	0.013	0.11	-	0.013
2559	26.7	2.25	0.014	0.071	0.01	-
2569	25.5	2.17	0.019	0.086	0.07	-
2574	8.36	1.09	0.026	0.12	0.03	-
2576	10.4	1.29	0.022	0.043	<0.01	-
2579	24.2	2.11	0.015	0.064	0.07	-
2580	26.2	1.93	0.021	0.071	0.05	-
2584	8.09	1.16	0.017	0.077	<0.01	-
2585	25.3	2.20	0.017	0.065	0.02	0.003
2593	27.8	2.10	0.015	0.070	0.03	0.005
2594	25.4	2.20	0.013	0.10	0.02	0.042
2596	24.1	2.24	0.012	0.093	0.03	0.020

Table 2 (cont'd)

Melt No.	Al	Cu	Mg	Fe	Si	Ti
2597	26.2	2.28	0.015	0.11	0.02	0.008
2599	26.8	2.21	0.012	0.11	0.03	0.065
2600-1	27.8	2.10	0.015	0.067	0.02	-
2600-2	30.7	2.11	0.014	0.067	0.02	0.069
2602-1	27.6	2.10	0.014	-	-	-
2602-2	27.1	2.14	0.015	-	-	0.048
2606-1	31.4	2.09	0.014	0.063	0.01	-
2606-2	27.4	2.18	0.018	0.063	0.01	0.022
2621-1	27.6	2.06	0.018	0.087	0.01	-
2621-2	27.8	2.06	0.018	0.087	0.01	0.004
2625-1	26.7	2.32	0.013	0.012	<0.01	-
2625-2	27.7	2.32	0.013	0.012	<0.01	0.025
2626-1	26.5	2.15	0.016	0.012	<0.01	-
2626-2	27.6	2.15	0.016	0.012	<0.01	0.032
2627-1	26.1	2.32	0.017	0.13	<0.01	-
2627-2	27.1	1.94	0.017	0.13	<0.01	0.047
2629-1	10.9	1.13	0.018	0.034	<0.01	-
2629-2	10.4	1.13	0.018	0.034	<0.01	0.029
2630-1	8.26	1.20	0.018	0.037	-	-
2630-2	8.19	1.01	0.018	0.037	-	<0.001
2633-1	10.7	1.29	0.023	0.03	<0.01	-
2633-2	11.1	1.29	0.023	0.03	<0.01	<0.001
2640-1	27.5	2.15	0.016	0.10	-	-
2640-2	27.0	2.15	0.016	0.10	-	0.014
2640-3	25.9	2.15	0.016	0.10	-	0.077
2645-1	26.3	2.16	0.014	0.03		
2645-2	25.6	2.16	0.014	0.03		0.016
2663-1	25.2	2.28	0.017	0.12	0.01	-

*Balance zinc.

<0.002% Pb, <0.002% Cd, <0.002% Sn.

Table 3 - Data from cooling curves.

Melt No.	Aluminum content wt %	Liquidus temp °C		Solidus temp °C		Eutectoid temp °C		Solidification range	
		Present data	Phase diagram	Present data	Phase diagram	Present data	Phase diagram	Present data	Phase diagram
2574	8	403	392	382	380	260	275	21	12
2555	11	422	416	382	380	262	275	40	36
2569	27	492	490	380	380	268	275	112	110

Table 4 - Effects of gating ratio and titanium modification on casting quality of the 2% Al alloy.

Melt No.	Sprue exit diam	Runner cross-section	Ingate cross-section	Gating ratio	Pouring temp °C	Pouring time s	Comments
2456	16 mm (5/8 in.)	25 x 25 mm ▸ 25 x 13 mm (1 x 1 in. ▸ 1 x 1/2 in.)	19 x 8 mm (3/4 x 5/16 in.)	1:3:3	540	10	Wide ring type shrinkage patterns.
2459	16 mm (5/8 in.)	25 x 25 mm ▸ 25 x 13 mm (1 x 1 in. ▸ 1 x 1/2 in.)	19 x 8 mm (3/4 x 5/16 in.)	1:3:3	540	13	Wide ring type shrinkage pattern.
2593	16 mm (5/8 in.)	25 x 25 mm ▸ 25 x 13 mm (1 x 1 in. ▸ 1 x 1/2 in.)	19 x 8 mm (3/4 x 5/16 in.)	1:3:3	558	-	Wide ring type shrinkage pattern in the unmodified alloy. Ring type patterns are closely spaced in Ti-modified condition.
2594	16 mm (5/8 in.)	25 x 25 mm ▸ 25 x 13 mm (1 x 1 in. ▸ 1 x 1/2 in.)	19 x 8 mm (3/4 x 5/16 in.)	1:3:3	550	-	Ring type patterns are clearly spaced after Ti-modification.
2596	16 mm (5/8 in.)	25 x 25 mm ▸ 25 x 13 mm (1 x 1 in. ▸ 1 x 1/2 in.)	19 x 8 mm (3/4 x 5/16 in.)	1:3:3	550	-	Ring type patterns are closely spaced after Ti-modification. Casting quality appears to be better than #2594.
2597	13 mm (1/2 in.)	25 x 25 mm ▸ 25 x 13 mm (1 x 1 in. ▸ 1 x 1/2 in.)	19 x 8 mm (3/4 x 5/16 in.)	1:5:5	560	-	Repetition of melt 2594 except that the gating ratio has changed. Shrinkage defects are not very deep. Casting quality appears to be better than #2594 and 2596 (Fig. 16).
2599	13 mm (1/2 in.)	25 x 25 mm ▸ 25 x 13 mm (1 x 1 in. ▸ 1 x 1/2 in.)	19 x 6 mm (3/4 x 1/4 in.)	1:5:4	560	21	Casting quality appears to be worse than #2597. Even the un-modified plate appears better than the Ti-modified plate.

Table 4 (cont'd)

Melt No.	Sprue exit diam	Runner cross-section	Ingate cross-section	Gating ratio	Pouring temp °C	Pouring time s	Comments
2600	13 mm (1/2 in.)	25 x 25 mm ▸ 25 x 13 mm (1 x 1 in. ▸ 1 x 1/2 in.)	19 x 6 mm (3/4 x 1/4 in.)	1:5:4	560	17	Casting quality has improved compared to #2599. Ti-modified plate appears better than the un-modified plate (Fig. 17).
2602	13 mm (1/2 in.)	25 x 25 mm ▸ 25 x 13 mm (1 x 1 in. ▸ 1 x 1/2 in.)	19 x 5 mm (3/4 x 3/16 in.)	1:5:3	555	18	Ti-modified appears better than the un-modified plate. Casting quality is much better. Practically no shrinkage defects (Fig. 18).
2606	13 mm (1/2 in.)	25 x 25 mm ▸ 25 x 13 mm (1 x 1 in. ▸ 1 x 1/2 in.)	19 x 10 mm (3/4 x 3/8 in.)	1:5:6	562	18.5	Casting quality appears very poor even after Ti-modification (Fig. 19).
2626	13 mm (1/2 in.)	25 x 25 mm ▸ 25 x 13 mm (1 x 1 in. ▸ 1 x 1/2 in.)	13 x 5 mm (1/2 x 3/16 in.)	1:5:2	530	24	Ti-modified plate appears worse than the un-modified plate. Shrinkage defects are not very deep.
2627	13 mm (1/2 in.)	25 x 25 mm ▸ 25 x 13 mm (1 x 1 in. ▸ 1 x 1/2 in.)	19 x 5 mm (3/4 x 3/16 in.)	1:5:3	537	19	Ti-modified plate appears better than the un-modified plate. Shrinkage defects not very deep. Casting quality is worse than #2602 for similar gating ratios.
2640	13 mm (1/2 in.)	25 x 25 mm ▸ 25 x 13 mm (1 x 1 in. ▸ 1 x 1/2 in.)	19 x 5 mm (3/4 x 3/16 in.)	1:5:3	553	18	Un-modified plate shows widely shaped ring type underside shrinkage. Ring-type patterns are closely spaced with 0.05% Ti addition, but appear little deep. 0.01% Ti addition again produces closely spaced defects which do not appear deep.
2658	13 mm (1/2 in.)	25 x 25 mm ▸ 25 x 13 mm (1 x 1 in. ▸ 1 x 1/2 in.)	19 x 5 mm (3/4 x 3/16 in.)	1:5:3	547	18	220 x 152 mm chill, tapered from 19 to 6 mm was placed on one plate. 63 mm diam riser placed on one end (Fig. 20). Chill area appears sound. Unchilled part shows lot of underside shrinkage for both un-modified and Ti-modified conditions (Fig. 21).
2663	13 mm (1/2 in.)	25 x 25 mm ▸ 25 x 13 mm (1 x 1 in. ▸ 1 x 1/2 in.)	19 x 5 mm (3/4 x 3/16 in.)	1:5:3	550	18	152 x 76 x 25 mm steel chill placed on either end of plate. 63 mm diam riser (with insulated sleeve) at centre. Plates are sound and no underside shrinkage.

Table 5 - Mechanical and physical properties of Zn-Al foundry alloys containing 8% Al.

Melt No.	wt % Al	Specimen condition	UTS MPa	0.2% YS MPa	0.5% YS MPa	% Elong in 4P	Density g/mm^3	Hardness HRB
2537	8.81	as-cast	248	206	219	1.4	6.303	57.3
2630	8.26	as-cast	252	200	216	1.5	6.297	57.2
2630	8.19	cast + Ti	233	192	200	1.0	6.322	53.2
Specification for ZA-8	8-8.8	as-cast	248-276	193-200	-	1.2	6.3	-

Table 6 - Mechanical and physical properties of Zn-Al foundry alloys containing 11% Al.

Melt No.	wt % Al	Specimen condition	UTS MPa	0.2% YS MPa	0.5% YS MPa	% Elong in 4P	Density g/mm^3	Hardness HRB
2448	10.6	as-cast	276	222	229	1.7	6.233	-
2449	12.6	as-cast	302	245	247	1.5	6.025	61.6
2482	10.95	as-cast	294	227	232	1.4	6.116	59.4
2529	11.55	as-cast	309	245	241	2.0	6.026	61.5
2539	11.60	as-cast	298	235	242	1.6	6.041	62.1
2576	10.4	as-cast	283	225	236	1.6	6.141	60.7
2629	10.9	as-cast	299	230	238	1.5	6.059	61.0
2629	10.4	cast + 0.029 Ti	275	218	228	1.0	6.090	59.1
Specification for ZA-12	10.5-11.5	as-cast	276-310	207-213	-	1-3	6.03	-

Table 7 - Mechanical and physical properties of Zn-Al foundry alloys containing 27% Al.

Melt No.	wt % Al	Specimen condition	UTS MPa	0.2% YS MPa	0.5% YS MPa	% Elong in 4D	Density g/mm^3	Hardness HRB
2456	30.6	as-cast	411	347	319	2.4	4.979	66.0
2456	30.6	cast + HT*	327	283	276	4.9	4.976	50.0
2459	29.6	as-cast	404	337	311	3.5	5.000	67.0
2459	29.6	cast + HT*	327	279	274	4.1	5.005	53.0
2476	28.9	as-cast	399	332	302	2.0	5.018	69.2
2476	28.9	cast + HT*	351	323	291	2.0	5.021	64.1
2527	28.66	as-cast	392	333	305	2.0	4.954	69.2
2527	28.66	cast + HT*	316	274	269	2.6	4.964	53.4
2531	29.12	as-cast	419	358	320	3.5	4.889	69.0
2531	29.12	cast + HT*	329	277	271	6.2	4.908	52.5
2543	27.0	as-cast	402	333	305	2.3	4.972	71.0
2593†	27.8	as-cast	407	-	-	3.6	5.042	70.8
2593†	27.8	cast + 0.005 Ti	398	-	-	2.8	5.032	70.4
2594†	25.4	cast + 0.042 Ti	403	-	-	4.0	5.103	70.5
2596†	24.1	cast + 0.002 Ti	397	-	-	3.0	5.059	70.3
2627	26.1	as-cast	386	328	306	1.5	5.032	70.4
2627	27.1	cast + 0.047 Ti	359	311	298	1.5	5.076	68.0
Specification for ZA-27	25-28	as-cast	400-441	365-372	-	3-6	5.000	-
		cast + HT*	310-324	255	-	8-11	5.000	-

*320°C, 3 h, furnace cool to room temperature.

†Extensometer was not used.

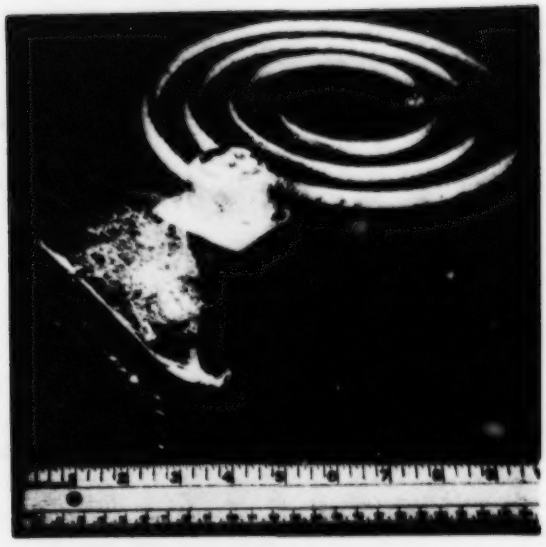

Fig. 1. Fluidity spiral (bottom view). (neg 8051)

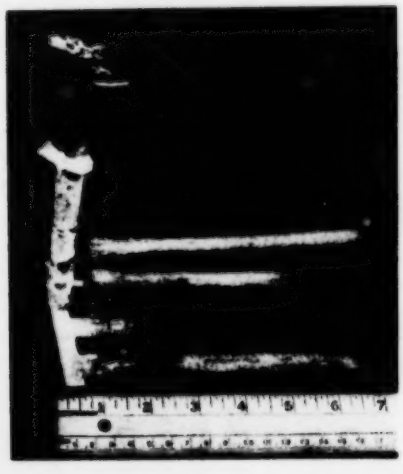

Fig. 2. Fluidity test pattern. (neg 8054)

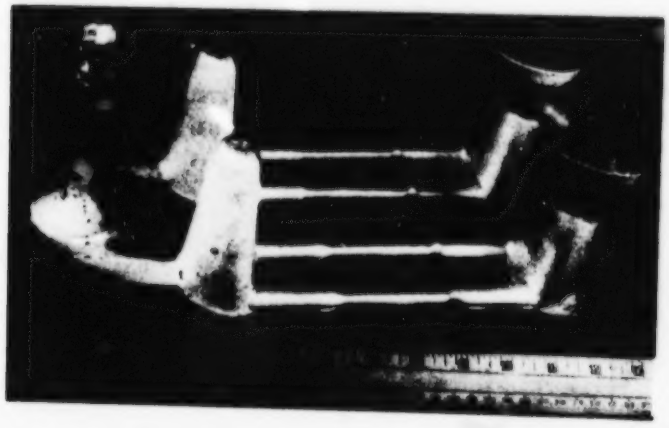

Fig. 3. Dow test bars with pouring sprue, gates and risers. (neg 8053)

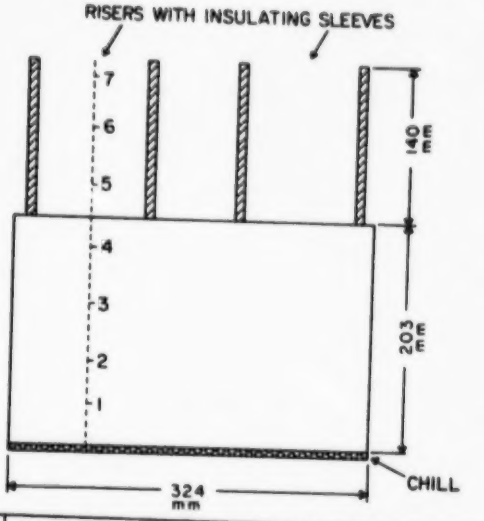

MELT No.	ALUMINUM CONTENT, Wt %, At							Alloy Type	Wt % Al added
	1	2	3	4	5	6	7		
2574	8.36	6.60	6.94	8.04	9.01	9.94	10.80	8%Al	8.0
2555	11.70	10.8	8.12	11.40	12.50	12.60	12.40	11%Al	11.4
2559	26.70	21.4	26.80	28.80	29.10	29.40	29.70	27%Al	26.0
2569	25.50	25.0	22.66	25.90	26.50	29.90	28.20	27%Al	26.0

Fig. 4. Schematic representation of the 133 x 203 x 324 mm block casting and the risers to show approximate locations for aluminum analysis. The table gives the aluminum contents for the three zinc-aluminum alloys. (neg 8724)

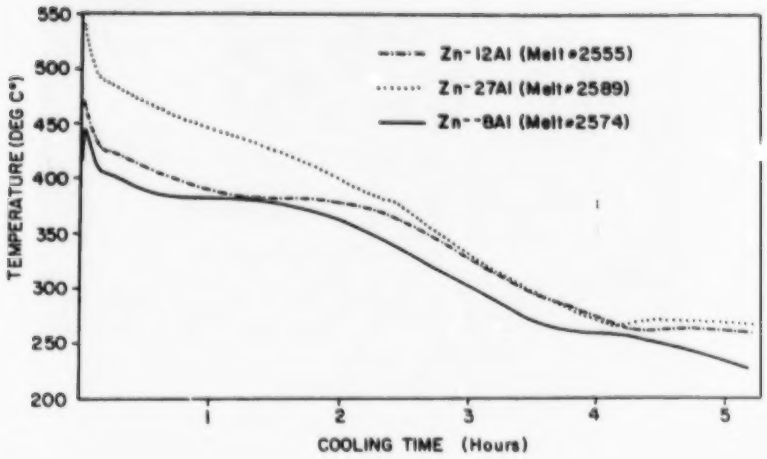

Fig. 5. Cooling curves for 8, 12 and 27% Al alloys obtained from 133 x 203 x 324 mm blocks. (neg 8726)

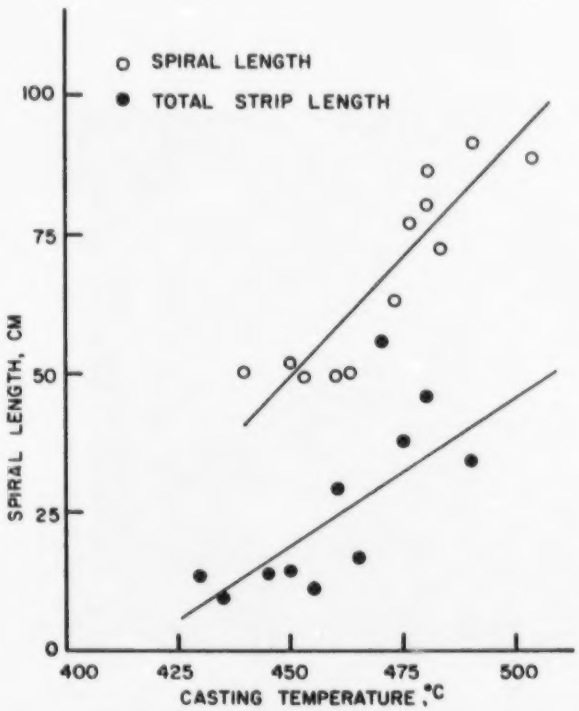

Fig. 6. Casting fluidity as a function of pouring temperature for the 8% Al alloy. (neg 8721)

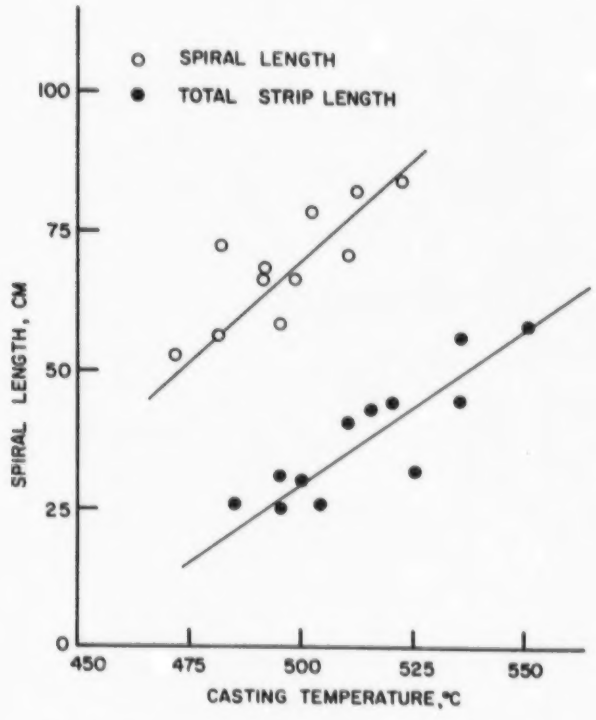

Fig. 7. Casting fluidity as a function of pouring temperature for the 11% Al alloy. (neg 8728)

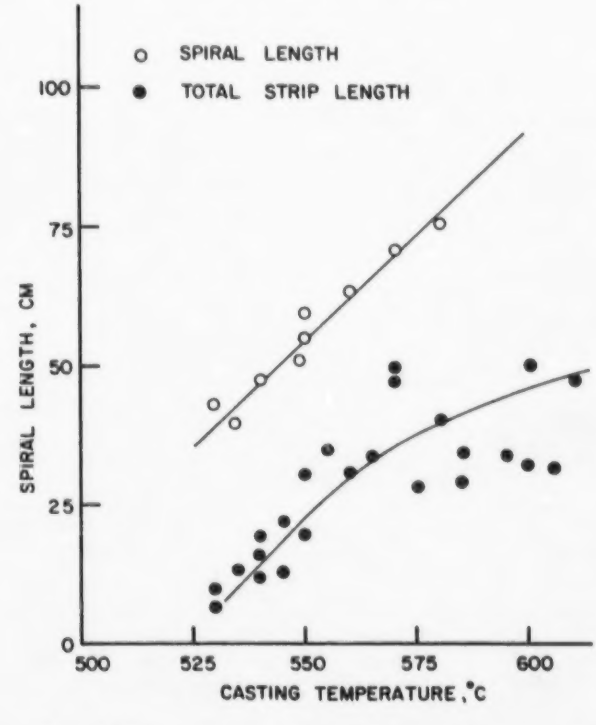

Fig. 8. Casting fluidity as a function of pouring temperature for the 27% Al alloy. (neg 8722)

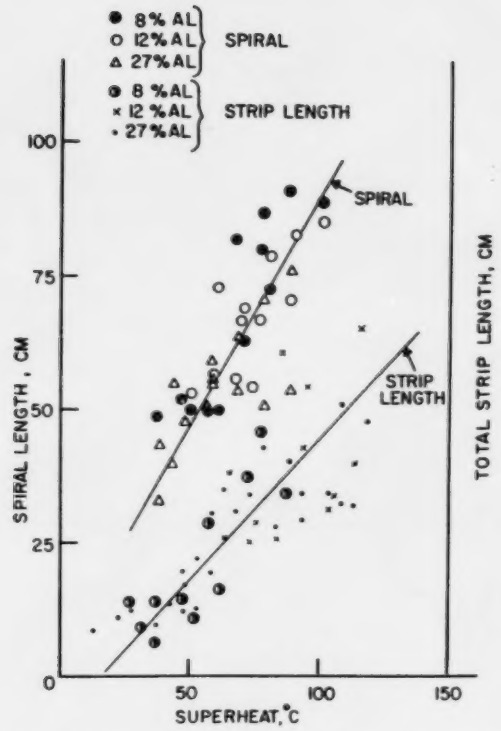

Fig. 9. Casting fluidity as a function of superheat for the 8, 11 and 27% Al alloys. (neg 8720)

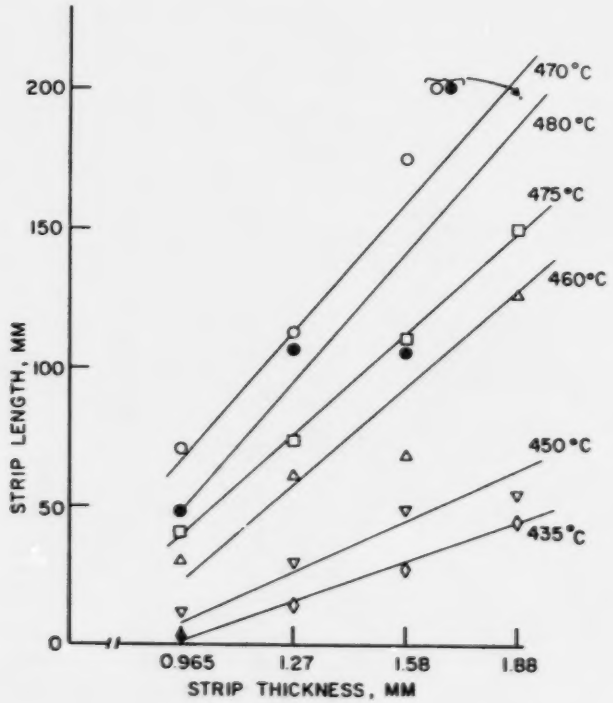

Fig. 10. Effect of strip thickness on strip length of the 8% Al alloy at various pouring temperatures. (neg 8725)

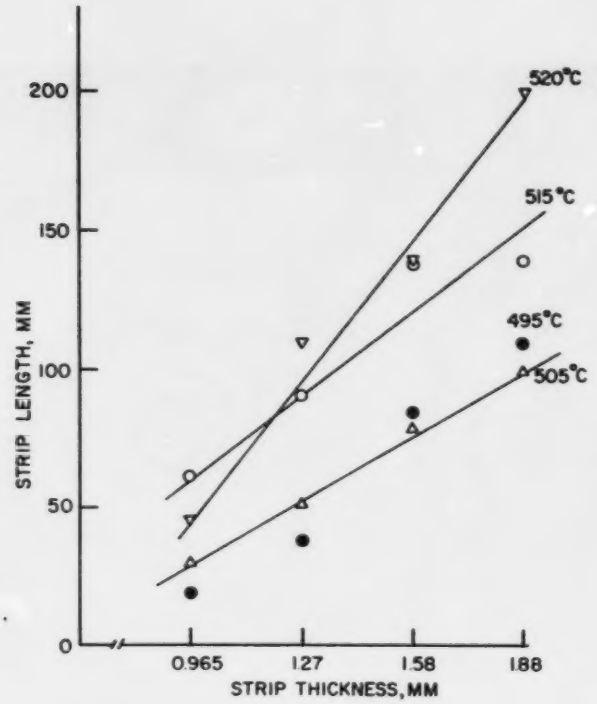

Fig. 11. Effect of strip thickness on strip length of the 11% Al alloy at various pouring temperatures. (neg 8727)

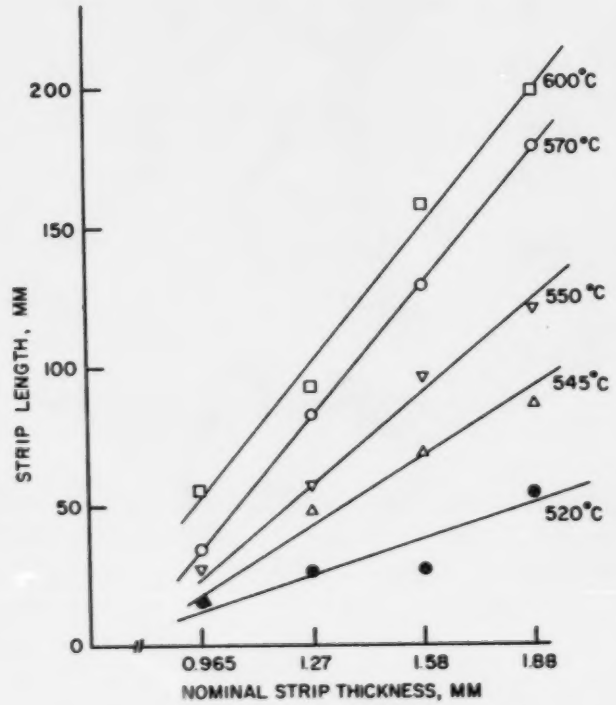

Fig. 12. Effect of strip thickness on strip length of the 27% Al alloy at various pouring temperatures. (neg 8723)

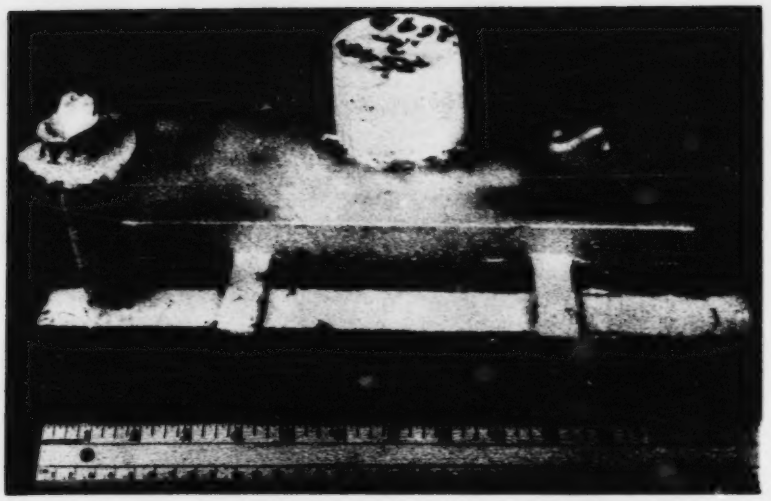

Fig. 13. 25 x 152 x 304 mm plate casting with the sprue, runner and ingates. Plate from the other side of the runner has been removed. Gating ratio of 1:5:3. (neg 8052)

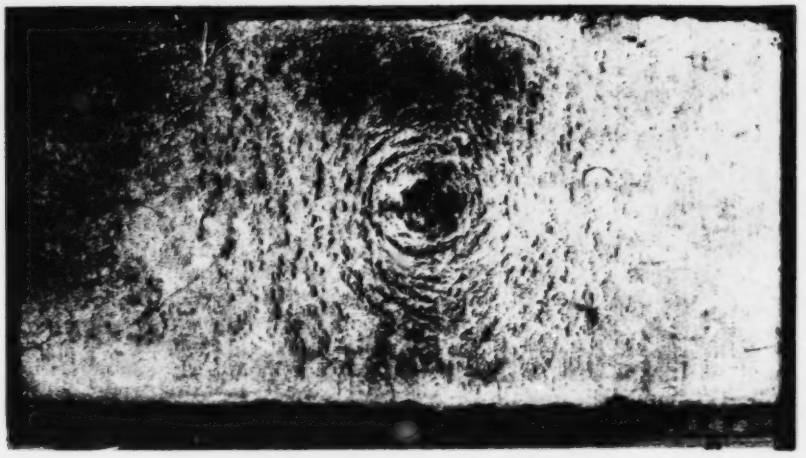

Fig. 14. Underside shrinkage defects on the drag side of the plate in melt No. 2459-3. Gating ratio of 1:3:3. (neg 7139)

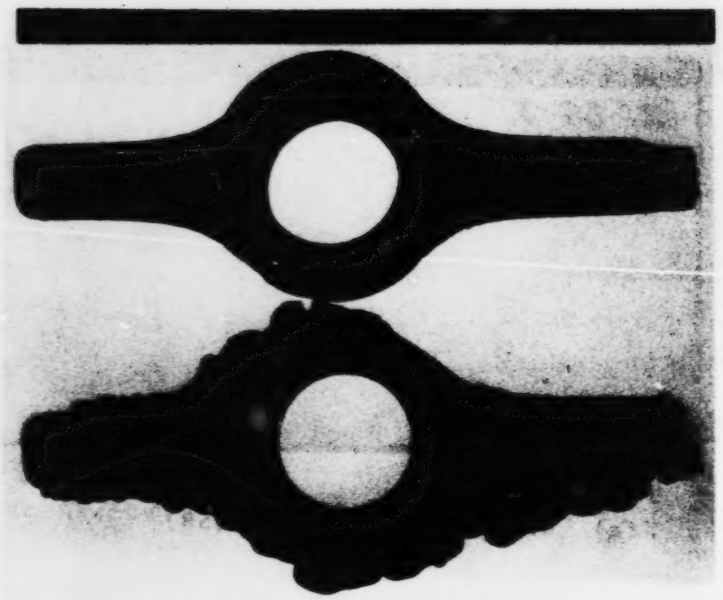

Fig. 15. Underside shrinkage in a typical commercial casting. Ingate cross-sectional area was reduced in the bottom casting. (neg 7547)

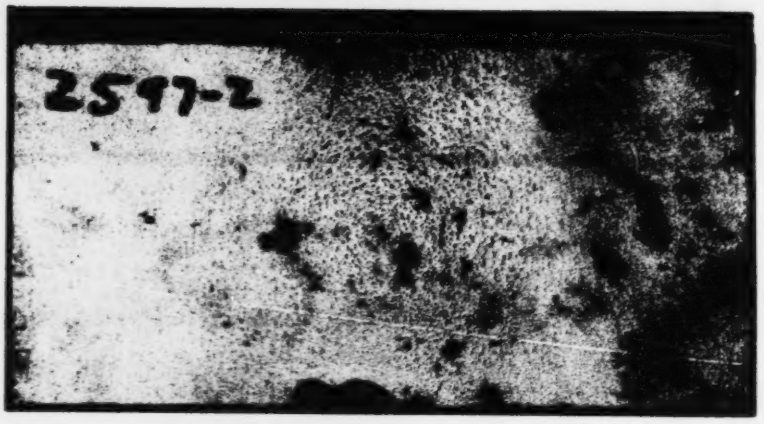

Fig. 16. Underside shrinkage in Zn-27% Al plate casting. Gating ratio of 1:5:5. 0.008% Ti. (neg 8065)

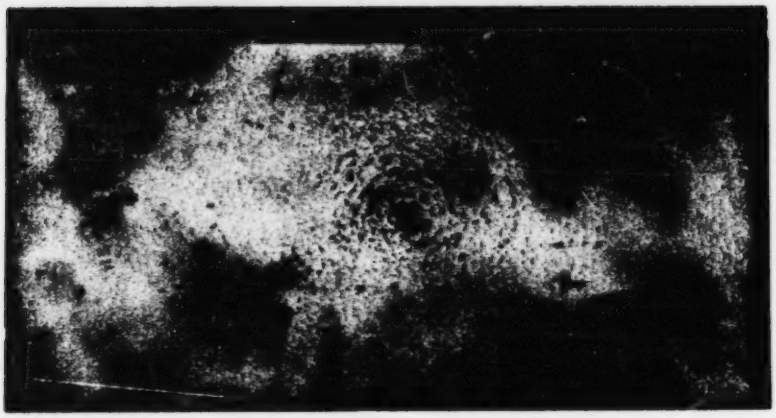

(a) unmodified. (neg 8058)

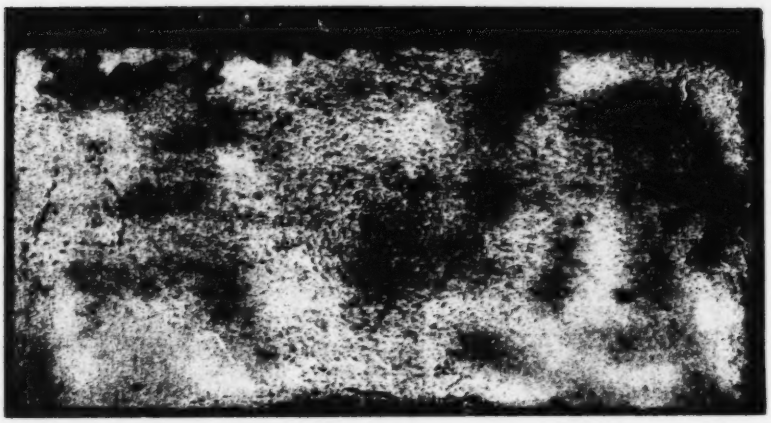

(b) 0.069% Ti.(neg 8062)

Fig. 17. Underside shrinkage in Zn-27% Al plate casting. Gating ratio of 1:5:4.

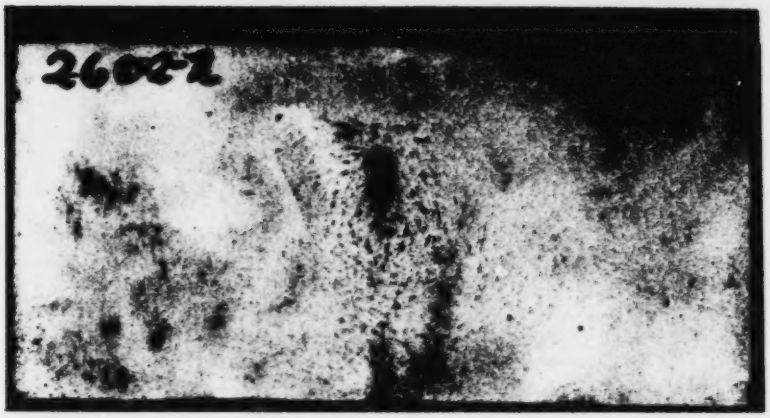

(a) unmodified. (neg 8061)

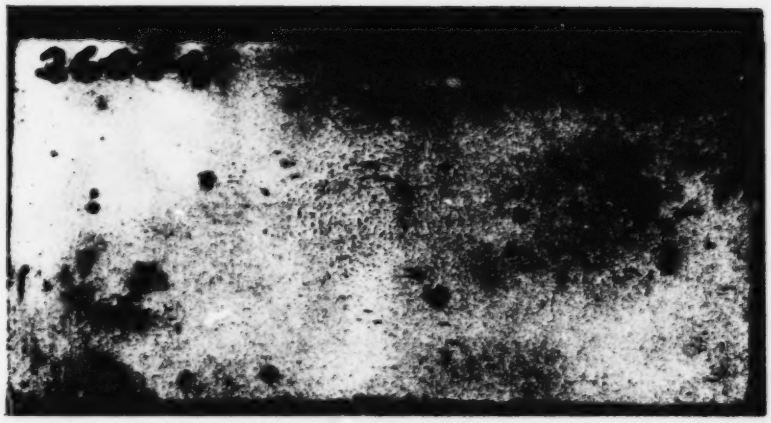

(b) 0.048% Ti. (neg 8059)

Fig. 18. Underside shrinkage in Zn-27% Al plate casting. Gating ratio of 1:5:3.

(a) unmodified. (neg 8055)

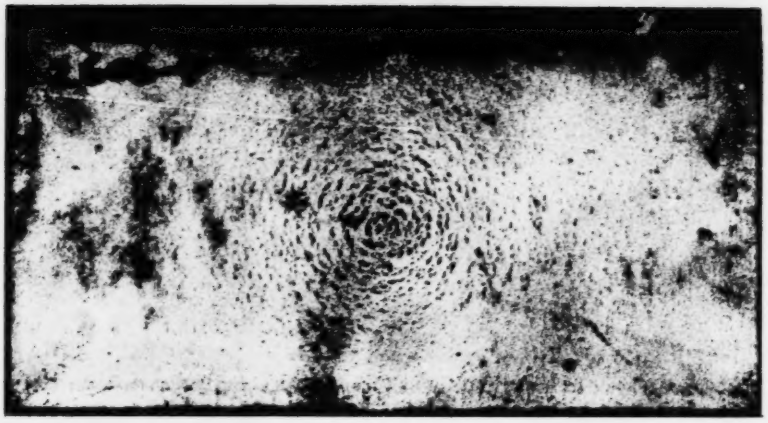

(b) 0.05% Ti. (neg 8064)

Fig. 19. Underside shrinkage in Zn-27% Al plate casting. Gating ratio of 1:5:6.

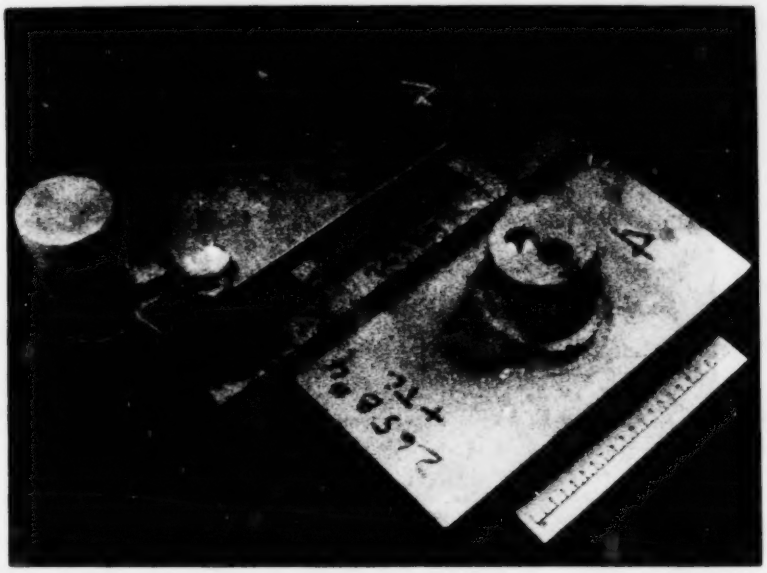

Fig. 20. Tapered chill was placed on the plate with end riser. Gating ratio 1:5:3. (neg 8135)

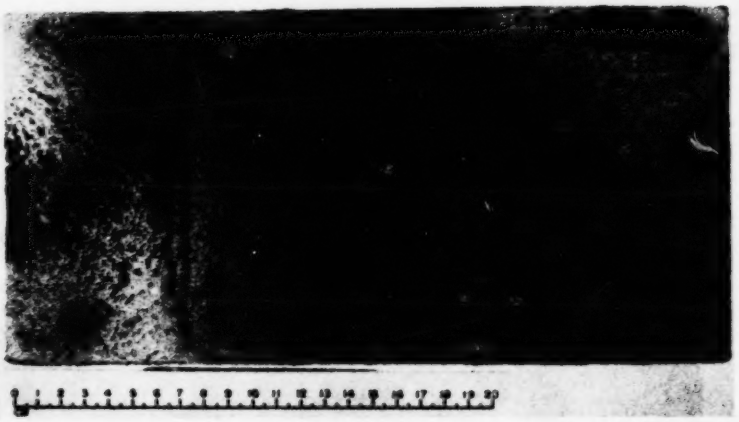

Fig. 21. Underside shrinkage in the unchilled area. (neg 8350)

(a) 2537-6-3, 8.81% Al, as-cast. X200 (neg 8308)

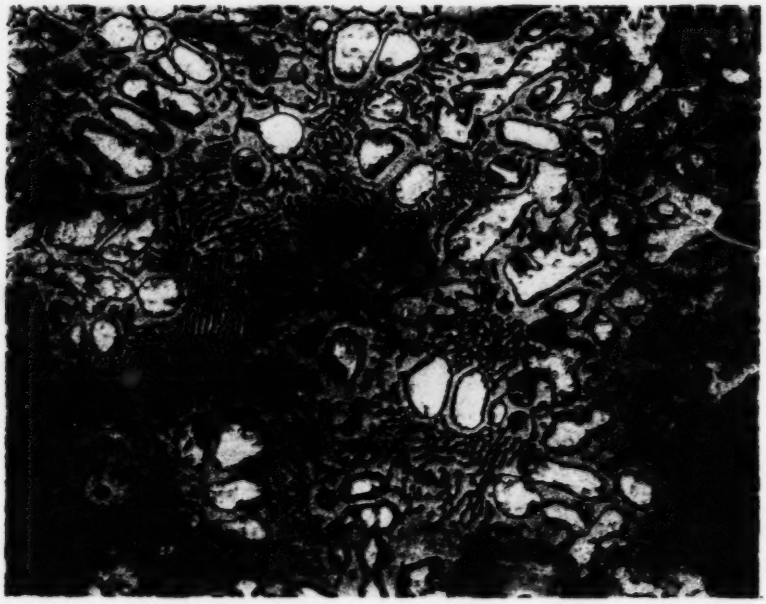

(b) 2482-4-4, 10.95% Al, as-cast. X200 (neg 8309)

Fig. 22 cont'd.

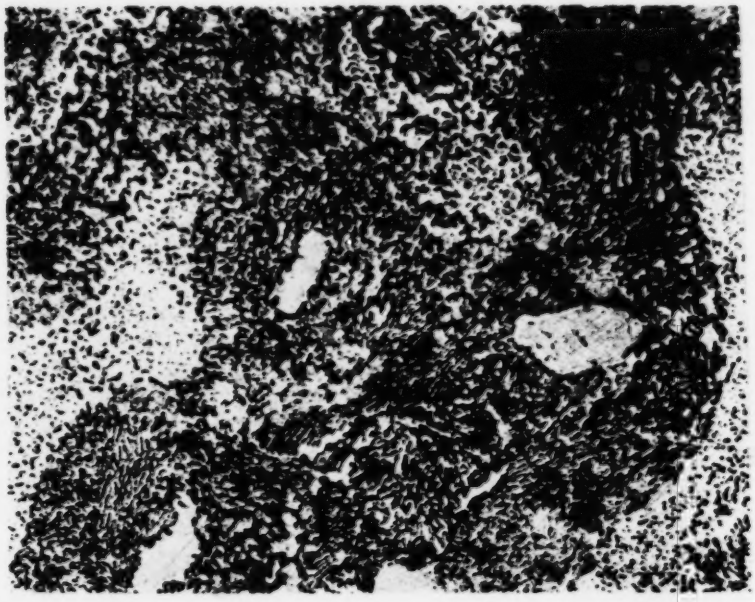

(c) 2459-2-1, 29.6% Al, as-cast. X1000 (neg 8306)

(d) 2459-2-3, 29.6% Al, cast + 320°C, 3 h, furnace cooled. X1000 (neg 8307)

Fig. 22. Optical micrographs of 8%, 11% and 27% Zn-Al foundry alloys. Etched in a solution containing 50 g Cr_2O_3, 4 g Na_2SO_4 and 100 ml H_2O.

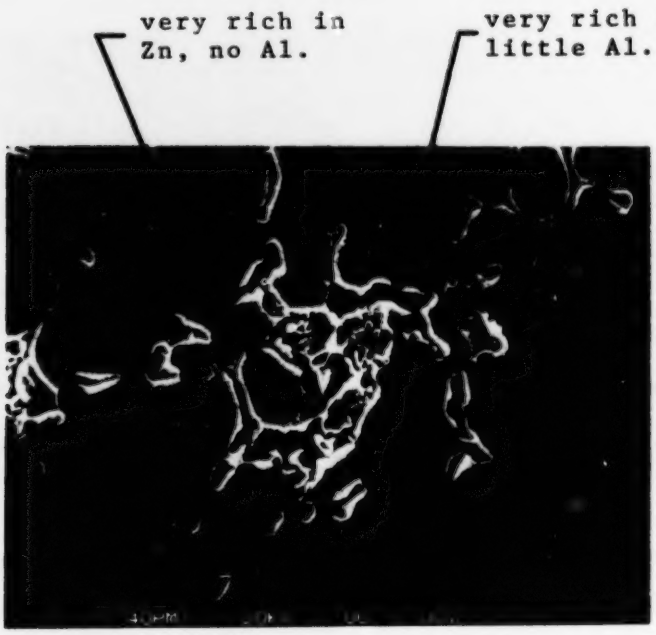

(a) Alloy 2593-3-3, titanium - modified. (neg 7921)

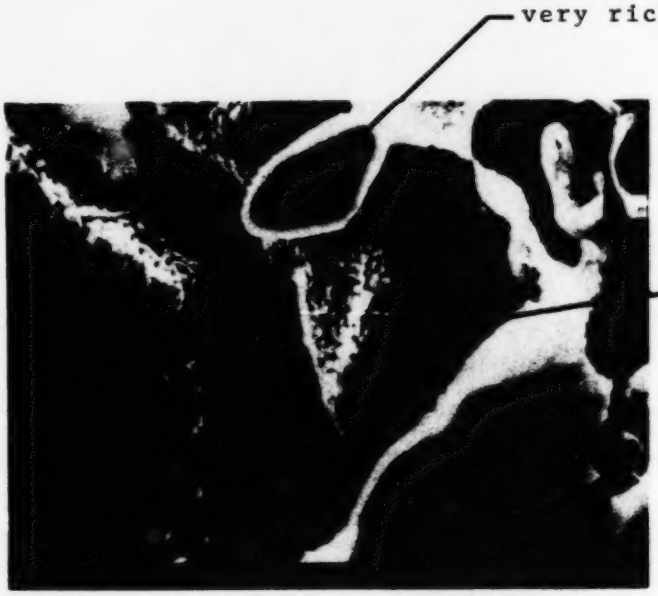
very rich in Zn, no evidence of Ti, relatively high Cu and low Al compared with Al-rich primary phase
low in Zn, high in Al (but less than Al-rich primary), very low in Cu. (neg 7918)

(b) Alloy 2593-3-3, titanium - modified. (neg 7918)

Fig. 23. cont'd.

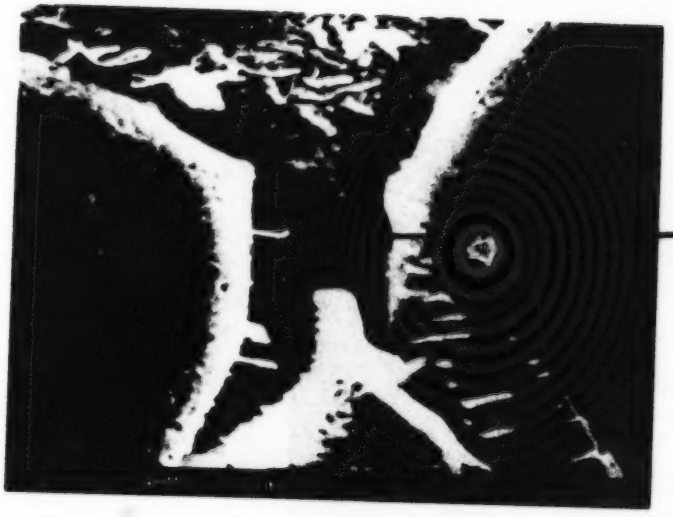

(d) alloy 2593-1-1. Unmodified. (neg 7920)

Fig. 23 cont'd.

(e) alloy 2594-1-1, 0.043% Ti. (neg 7922)

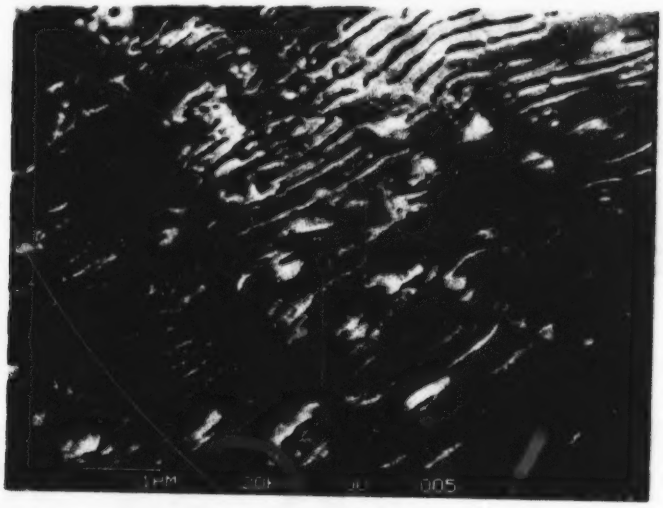

(f) alloy 2594-1-1, 0.043% Ti. (neg 7924)

Fig. 23 cont'd.

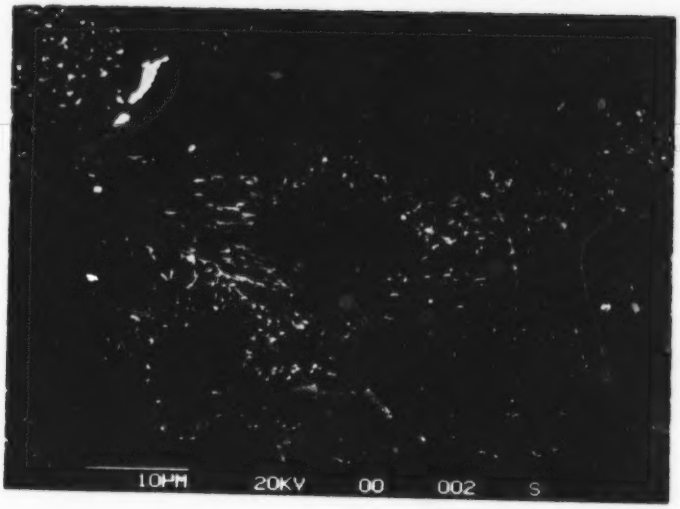

(g) alloy 2596-1-1, 0.02% Ti. (neg 7938)

Fig. 23. Scanning electron micrographs of unmodified and titanium-modified Zn-27% Al alloys. Etched in a solution containing 50 g Cr_2O_3, 4 g Na_2SO_4 and 100 ml H_2O.